Propeller tip vortex cavitation mitigation using roughness

VIII International Conference on Computational Methods in Marine Engineering
MARINE 2019
R. Bensow and J. Ringsberg (Eds)

PROPELLER TIP VORTEX CAVITATION MITIGATION USING ROUGHNESS

Abolfazl Asnaghi*, Urban Svennberg†, Robert Gustafsson† and Rickard E. Bensow*

*Department of Mechanics and Maritime Sciences, Chalmers University of Technology, Sweden
e-mail: asnaghi@chalmers.se, rickard.bensow@chalmers.se

† Rolls-Royce Hydrodynamic Research Center, Rolls-Royce AB, Kristinehamn, Sweden
e-mail: urban.svennberg@rolls-royce.com, robert.gustafsson@rolls-royce.com

Abstract. This paper presents an investigation of roughness application on marine propellers in order to alter their tip vortex properties, and consequently mitigate tip vortex cavitation. SST $k-\omega$ model along with a curvature correction is employed to simulate the flow on an appropriate grid resolution for tip vortex propagation, at least 32 cells per vortex diameter. The roughness is modelled by using a rough wall function to increase the turbulent properties in roughed areas. In one case, roughness geometry is included as a part of the blade geometry, and the flow around them are resolved. To minimize the negative effects of the roughness on the propeller performance, the roughness area is optimized by simultaneous consideration of the tip vortex mitigation and performance degradation. For the considered operating condition, it is found that having roughness on the tip region of suction side can reduce the cavitation inception by 18 % while keeping the performance degradation in a reasonable range, less than 2%.

Key words: Cavitation, Mitigation, Tip Vortex, Inception, CFD

1 INTRODUCTION

Tip vortex cavitation (TVC) is usually the first type of cavitation that appears on a propeller. Therefore, it is considered as the main controlled cavitation characteristics in the design procedure of low-noise propellers, where their operating profiles require very low radiated noise emissions. Several approaches are proposed and tested to modify tip vortex structures in order to prevent or at least delay tip vortex cavitation inception. Among these approaches, the application of roughness is a promising way [1]. Surface roughness affects the tip vortex roll-up as the roughness elements promote transition to turbulence in laminar boundary layers and therefore alter the near-wall flow structures. If size, pattern, and location of roughness elements are selected appropriately, the alteration can lead to tip vortex breakdown, and consequently lead to TVC mitigation.

The selected propeller is from a research series of highly skewed propellers having a low effective tip load and is typical for yachts and cruise ships, where it is very important to suppress

and limit propeller-induced vibration and noise. In this type of propellers, the main source of noise and vibration is the vortex cavitation in the tip region. In our previous studies, numerical simulations of tip vortex flows around this propeller having smooth blades were carried out and successfully compared with experimental measurements [2]. The aim of the present study is to provide further knowledge about the effects of the surface roughness on the TVC and the possibility of using roughness to delay the cavitation inception.

The tip vortex flows around the propeller are simulated by the two equation SST $k-\omega$ model of OpenFOAM on appropriate grid resolutions for tip vortex propagation, at least 32 cells per vortex diameter according to previous studies guidelines [3, 4]. The η_3 curvature correction method is employed to prevent overprediction of turbulent viscosity in highly swirling tip regions [5, 6].

The roughness is included in the simulations by employing two different approaches. In the first approach, rough wall functions are used to mimic the effects of roughness by increasing the turbulent properties in roughed areas [7] . The second approach modifies the mesh topology by removing cells in roughed areas to create random roughness elements. While the first approach models the roughness effects, the second one actually includes the geometry change into the simulations. However, as the roughness elements have very small sizes, resolving the flow around them demands a very fine mesh resolution.

Roughness application on different blade areas, e.g. suction side and pressure side are considered. It is evaluated how roughness alters the vortical structures on the blade and as a result in the tip vortex region. The analysis provides further knowledge on how roughness changes the flow pattern around the blade tip and mitigates the cavitation. The propeller performance degradation in different roughness conditions is computed and by considering the tip vortex cavitation inception improvement, the most optimum roughness pattern is proposed.

2 EQUATIONS

To model the roughness effect, the wall function developed by Tapia [8] for the inner region of the turbulent boundary layer or the log-law region (e.g. $11 \leq y^+$ in OpenFOAM wall functions) is used,

$$u^+ = \frac{1}{\kappa}\ln(Ey^+) - \Delta B, \tag{1}$$

with the von Karman constant $\kappa = 0.41$, the constant E=9.8, the dimensionless wall distance $y^+ = u_\tau y/\nu$, and the velocity shift correction ΔB due to the roughness elements. The nondimensional roughness height is presented by $K_s^+ = u_\tau K_s/\nu$ where K_s is the roughness height, $u_\tau = \sqrt{\tau_w/\rho}$ is the shear velocity, and τ_w is the wall shear stress. In this approach, the height of the elements should be smaller than the height of the cells adjacent to the wall, i.e. $K_s^+ \leq y^+$. Otherwise, the part of roughness elements located outside the adjacent cells will not be included in the modelling.

In a smooth regime represented by $K_s^+ \leq 2.5$, the correction ΔB is set to zero and the wall function recalls the smooth wall function. For a transitionally rough regime, $2.5 < K_s^+ < 90$, the correction reads,

$$\Delta B = \frac{1}{\kappa}\ln\left[\frac{K_s^+ - 2.25}{87.75} + C_s K_s^+\right]\sin\big(A\big), \tag{2}$$

where $A = 0.425[\ln(K_s^+) - 0.811]$, and C_s is a constant representing shape and form of roughness elements. It is suggested that C_s varies from 0.5 to 1 where $C_s = 0.5$ corresponds to the uniformly distributed sand grain roughness. If the roughness elements deviate from the sand grains, the constant roughness should be adjusted by comparing the results with experimental data.

For a fully rough regime having $90 \leq K_s^+$, the ΔB correction is represented by,

$$\Delta B = \frac{1}{\kappa}\ln\left[1 + C_s K_s^+\right]. \tag{3}$$

The turbulent viscosity of cells adjacent to the rough wall is then recalculated using the following formula,

$$\mu_t = \mu\left[\frac{y^+\kappa}{\ln(Ey^+/e^{\kappa\Delta B})} - 1\right]. \tag{4}$$

The flow is simulated by employing the SST $k-\omega$ model [3]. To include the effects of curvature correction, the production term of the ω equation is multiplied by F_{rc},

$$F_{rc} = 1 + \alpha_1 \mid \eta_3 \mid + 3\alpha_1\eta_3, \tag{5}$$

where $\alpha_1 = -0.2$, and $C_r = 2.0$. η_3 is a velocity gradient invariants [5],

$$\eta_1 = \bar{S}_{ij}^*\bar{S}_{ij}^*, \quad \eta_2 = \bar{\Omega}_{ij}^*\bar{\Omega}_{ij}^*, \quad \eta_3 = \eta_1 - \eta_2, \tag{6}$$

defined through the non-dimensional strain rate and rotational rate tensors,

$$\bar{S}_{ij}^* = \tau\bar{S}_{ij}, \quad \bar{\Omega}_{ij}^* = \tau\bar{\Omega}_{ij}^{mod}, \tag{7}$$

where the strain rate and rotational rate tensors are defined by,

$$\bar{S}_{ij} = \frac{1}{2}(\frac{\partial\bar{u}_i}{\partial x_j} + \frac{\partial\bar{u}_j}{\partial x_i}), \quad \bar{\Omega}_{ij} = \frac{1}{2}(\frac{\partial\bar{u}_i}{\partial x_j} - \frac{\partial\bar{u}_j}{\partial x_i}). \tag{8}$$

As can be seen, η_1 represents the non-dimensional strain rate magnitude, η_2 represents the non-dimensional vorticity magnitude, and η_3 is a linear combination of these two independent velocity-gradient invariants. Please refer to [3] for further information.

3 CASE DESCRIPTION

The basic design of the propeller is from a research series of five-bladed highly skewed propellers having low effective tip load where it is very important to suppress and limit propeller-induced vibration and noise. The main or first source of noise, for this type of propellers, is cavitation in the tip region.

The computational domain of the propeller is presented in Figure 1. The domain is simplified to a cylinder extending 4D upstream the propeller and 8D downstream of the propeller where D=0.2543 m is the diameter of the propeller. In order to model the moving mesh (i.e. relative motion between the propeller and the external domain), the computational domain has been decomposed into two regions connected to each other through AMI (Arbitrary Mesh Interpolation) boundaries. While the outer region is stationary, the rotation of the region close to the propeller where all interesting flow phenomena occur has been handled by MRF.

The simulations are conducted at a constant inlet velocity, a fixed pressure outlet boundary and the advance ratio of the propeller is then set by adjusting the rotational rate of the propeller. No-slip wall boundary condition is used for the propeller and the shaft. The outer cylinder boundary is set as a slip boundary to reduce the mesh resolution requirements far from the propeller. Then, the blockage effects are considered in comparing the numerical results with related experimental measurements. All of the simulations are conducted at one J value where the tip vortex forms on the suction side of the blade. The comparison between numerical simulations and the experimental measurements of the smooth propeller is presented and discussed in [2].

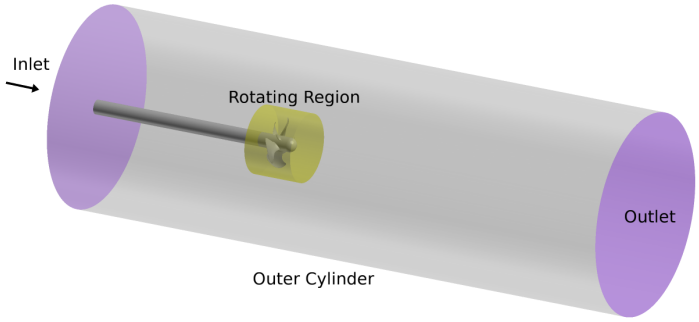

Figure 1: Computational domain of the propeller.

The distribution of the propeller mesh is presented in Figure 2. Different refinement boxes are applied to provide finer resolutions around the rotating propeller region, Figure 2a. The baseline mesh resolution on the blades gives x^+ and $z^+ < 250$, where finer resolutions are provided at the leading edge and trailing edge of the blades. Further finer resolution is achieved where tip refinement is applied. The nominal values given above are calculated based on the inlet velocity and the propeller diameter as the reference length and verified afterwords. The prismatic layers of the refined blad consists of 20 layers having extrusion factor of 1.15 where the first cell wall normal resolution is $y^+ = 35$.

The tip vortex refinement is applied on one blade only, where three helical shape refinement zones are defined based on the primary vortex trajectory. The refinement zones cover the tip of the blade, and therefore provide more refined grid resolutions on the tip of this blade, Figure 2b. These helical refinement regions provide spatial resolutions as fine as 0.2 mm, 0.1 mm, and 0.05 mm in H1, H2, and H3 regions, respectively.

The roughness pattern is tested on the suction side and pressure side of the refined blade tip, Figure 3. The study consist of the roughness modelling on the blade tip of the suction side, SS, of the pressure side, PS, and of the suction and pressure sides, SS+PS. The fully rough, FR, blade condition is also included. For one case where the roughness is only applied on the suction side tip region, the mesh topology is modified by removing cells to include the roughness elements into the simulations, Figure 3c. This will provide the opportunity to resolve the flow around these roughness elements.

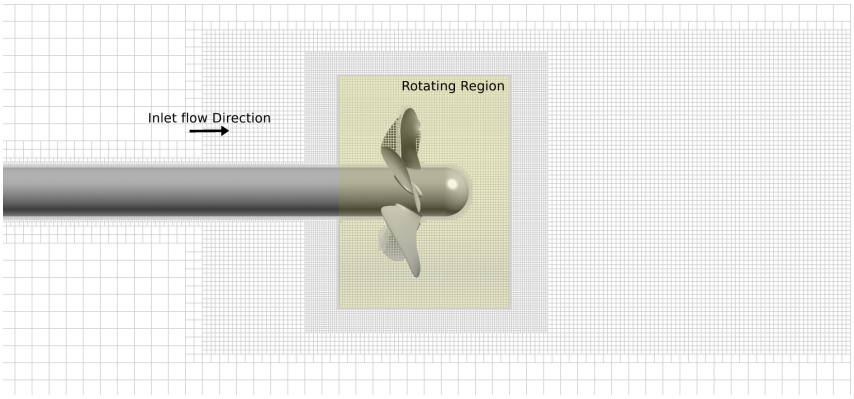

(a) Streamwise resolution

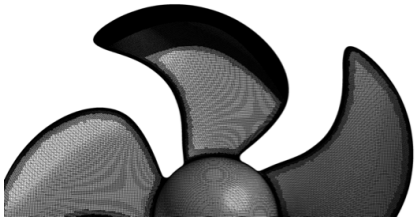

(b) Blade surface resolution

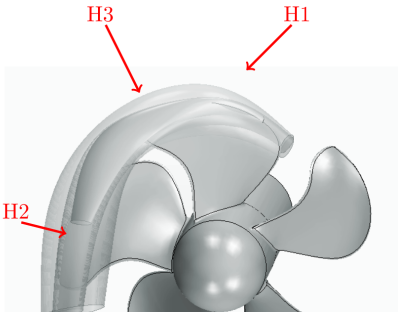

(c) Helical tip refinement

Figure 2: Mesh distribution of the propeller.

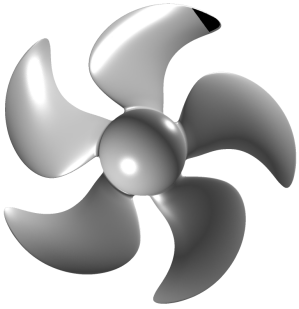

(a) Suction side view

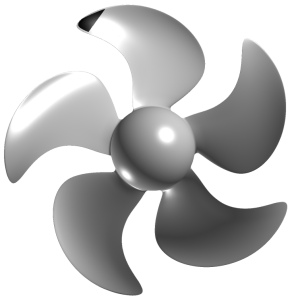

(b) Pressure side view

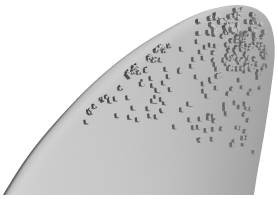

(c) Geometrical roughness

Figure 3: (a) and (b): Roughness areas on the suction side and pressure side of the refined blade; (c): distributions of roughness elements on the SS.

4 RESULTS

The numerical results are presented in two parts. In the first part, effects of having roughness on different areas of the blade are evaluated. It includes tip vortex cavitation inception

prediction, and also the propeller performance. The roughness size is selected to be equal to 250 μm and it is assumed that the roughness is distributed uniformly, i.e. $C_s = 0.5$. In the second part, for the case where the roughness is only applied on the suction side of the blade, the flow around the roughness elements are resolved.

4.1 Evaluation of roughness patterns

The performance of the propeller for different surface conditions are presented in Table 1. Thrust and torque coefficients as well as the efficiency, are presented relative to the smooth propeller condition. The results indicate an increase in the torque coefficient when roughness is included. The thrust coefficient, however, is more dependent on the roughness pattern. For the FR blade, the maximum thrust decrease, -13.4 %, and efficiency drop, -16.6 %, are observed. Having roughness on the PS leads to higher K_t but it also demands for higher K_q. This eventually results in a lower propeller efficiency, around -2.5 %. When roughness is only applied on the SS, the variation of the thrust and torque is minimum. Further quantitative justification of these results demands uncertainty analysis which has been postponed for future studies. The results, however, clearly confirm that in order to minimize the negative effects of roughness on the propeller performance, the roughness area should be optimized.

Table 1: Variation of thrust, torque and efficiency relative to the smooth foil condition for different roughness patterns. Refer to Figure 3 for descriptions of SS, PS, and SS+PS.

Case	K_t (%)	K_q (%)	Efficiency (%)
Smooth	–	–	–
SS	-0.8	0.2	-1.0
PS	1.2	3.8	-2.5
SS+PS	2.1	4.6	-2.4
FR	-13.4	3.8	-16.6

In Figure 4, the predicted cavitation inception based on the minimum pressure criterion is presented for different roughness patterns. As the propeller was not tested at the selected condition, the experimental data is extrapolated to this operating condition. Among the results, the FR condition has the lowest cavitation inception comparing to other patterns. The predicted cavitation inception in SS and SS+PS patterns is close to each other, and the difference between them is believed to lie in the uncertainty of the numerical results in the current simulations. The results indicate the necessity of having roughness on the side where the tip vortex forms, e.g. suction side in the evaluated operating condition. We also observed some stability and convergence issues with the simulations related to PS and SS+PS. These could be related to the flow gradients at the low quality cells on the edge of the blades at the interface of the prismatic layers and the volumetric cells. Another reason could be related to the nature of curvature correction model. The curvature correction reduces the turbulent viscosity and by that increases the formation of vortical structures and therefore increases the unsteadiness of the flow.

It is noted that compared to the LES simulations on the fully resolved resolution for the same operating condition of the smooth blade [2], the tip vortex is under predicted in the RANS

simulations. Where in LES simulations of fully resolved boundary layer resolution the cavitation inception is found to be around 7.4, for wall modelled RANS simulation the cavitation inception is around 5.5. This, however, is not a major issue in the current study, as the main objective is to compare different roughness patterns and to compare how the tip vortex forms on them rather than exact prediction of tip vortex.

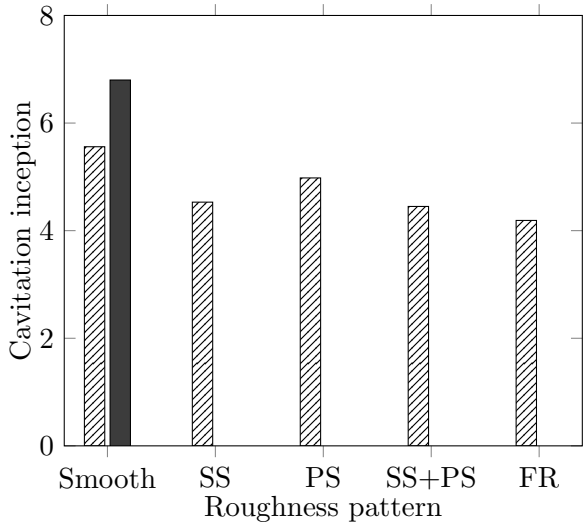

Figure 4: Variation of the cavitation inception versus different surface roughness areas, solid bar is the extrapolated experimental measurements for the smooth blade.

Among the studied cases, the lowest cavitation inception points belong to the FR blade, and then SS or SS+PS which have similar inception prediction. However, as the performance degradation is much lower in SS, this case is considered as the outcome of the roughness area optimization.

4.2 Evaluation of roughness modelling

Modelling of roughness with a wall function has some limitations, especially for the employed wall function where the roughness pattern is included into the CFD with only two representing values, i.e. roughness height and C_s. Depending on the topology of roughness elements, modelling them with an averaged value as sand grains may increase the deviation between numerical results and experimental observations. As a first attempt, in this section the numerical simulations of wall modelled roughness is compared with resolving the flow around the roughness elements.

In Figure 5 and 6, numerical results of resolved flow around the roughness elements are presented. The figures are the zoomed view of the blade having the roughness elements on its suction side where the blade is colored with the turbulent viscosity. The figures include the pressure iso-surface of the saturation pressure colored black, and the vortical structure based on Q=1000 presented with transparent gray color.

The low turbulent viscosity around the roughness elements indicates formation of vortical

structures around them. The location of these structures are predicted by the curvature correction model, and then the turbulent viscosity is lowered there to allow the flow development. This can be noted from Figure 6 where the distribution of Q is represented.

Formation of vortical structures around the roughness elements weakens the tip vortex, and mitigates the tip vortex cavitation inception. However, they lead to formation of several low pressure spots on the blade. These spots can intensify the cavitation on the blade as the roughness elements can easily introduce the nuclei into these low-pressure region. This poses the demand for the simultaneous analysis of cavitation inception in tip vortex and on the blade.

It should be noted that although the spatial resolution around the roughness elements is very coarse to accurately resolve the flow around them, it is still possible to decently predict their impact on the tip vortex.

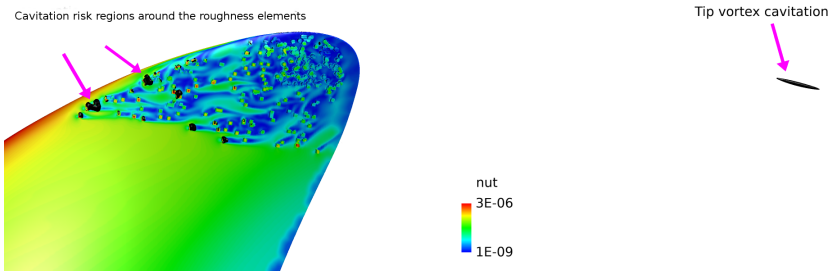

Figure 5: Distribution of the turbulent viscosity around the roughness elements along with the iso-surface of pressure colored black, zoomed view of the roughness elements on the SS.

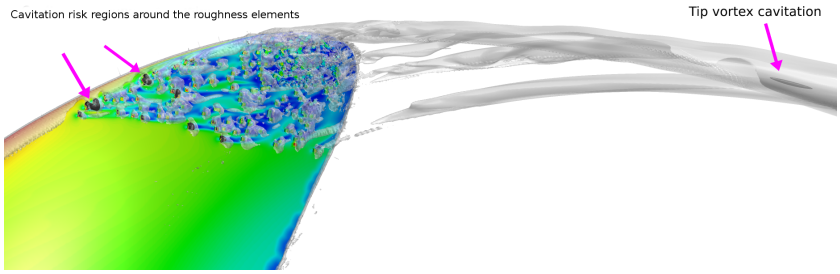

Figure 6: Distribution of the vortical structures around the roughness elements along with the iso-surface of pressure colored black, zoomed view of the roughness elements on the SS.

Table 2: Variation of thrust, torque and efficiency relative to the smooth foil condition for different roughness modelling approaches.

Case	K_t (%)	K_q (%)	Efficiency (%)
Smooth	–	–	–
SS Wall modelled	-0.8	0.2	-1.0
SS Roughness modelled	-1.9	0.1	-1.8

For the resolved flow around the roughness elements, the cavitation inception is found to be around 3.28 while with wall-modelling approach the predicted inception point is 4.53. Lower propeller performance is noted for the resolved flow as well, Table 2. When conducting a comparative analysis, e.g. comparing different patterns, the large difference between the cavitation inception predictions has less importance. But when it comes to find the balance between the cavitation tip vortex and the blade cavitation, the accurate prediction of flow around roughness elements is inevitable.

5 CONCLUSIONS

The results on the tested propeller show that the application of roughness can be a solution to mitigate a tip vortex. It is found that the area where the roughness is applied has a direct impact on the interactions between the roughness elements and boundary layers over the blade, and eventually on the strength of the tip vortex. The presence of roughness alters the boundary layer distribution and consequently affects the tip vortex formation and development. This leads to a weaker tip vortex, and mitigation of tip vortex cavitation.

It is noted that the negative effects of roughness on the propeller performance can be minimized when the roughness area is optimized. This can be done by considering different roughness patterns on the suction side and pressure side of the propeller. For the tested propeller having full rough blades, the performance efficiency drops 16.6 % while in the optimum roughness area the performance degradation can be kept below 2 %.

The difference between the cavitation inception predicted by the wall modelled roughness and resolved flow is found to be considerable where the predicted cavitation inception by wall modelled approach is 4.53 and for the resolved flow the inception point is 3.28. However, there are still some uncertainties about resolving the flow over the roughness elements by RANS modelling that demands for further investigations.

When the flow around the roughness elements are resolved, several low pressure spots on the blade are observed. These low pressure regions can lead to bubble or sheet cavitation on the blade. Therefore, the compromise between tip vortex and bubble cavitation is needed when roughness patterns are compared.

It is found that having roughness on the tip region of blade suction side is sufficient to mitigate the tip vortex and at the same time keep the performance degradation at a reasonable level. However, it should be considered that the current study focuses only on one operating condition where the tip vortex is formed on the suction side of the blade. To generalize the finding further studies with a wider range of operating conditions are necessary.

ACKNOWLEDGEMENTS

Financial support for this work has been provided by Vinnova through the RoughProp project, Grant number 2018-04085. The simulations were performed on resources at Chalmers Centre for Computational Science and Engineering (C3SE) provided by the Swedish National Infrastructure for Computing (SNIC).

REFERENCES

[1] Kruger, C. and Kornev, N. and Greitsch, L.*Influence of propeller tip roughness on tip vortex strength and propeller performance.* Ship Technology Research, 63(2):110120, 2016.

[2] Asnaghi, A. and Svennberg, U. and Bensow, R.E. *Numerical and experimental analysis of cavitation inception behaviour for high-skewed low-noise propellers*, Applied Ocean Research, 79:197214, 2018.

[3] Asnaghi, A.*Computational modelling for cavitation and tip vortex flows*, PhD -thesis, Chalmers University of Technology, 2018.

[4] Asnaghi, A. and Bensow, R.E. and Svennberg, U.*COMPARATIVE ANALYSIS OF TIP VORTEX FLOW USING RANS AND LES*, VII International Conference on Computational Methods in Marine Engineering, MARINE 2017At: Nantes, France, 2017.

[5] Arolla, S.K. *Modeling and eddy simulation of rotating and curved turbulent flows*, Doctoral Thesis, Iowa State University, Ames, Iowa, 2013.

[6] Arolla, S.K. and Durbin, P.A.*Modelling rotation and curvature effects within scalar eddy viscosity model framework*, Int. J. Heat Fluid Flow, 39 (1), 2013.

[7] Asnaghi, A. and Svennberg, U. and Gustafsson, R. and Bensow, R.E. *Roughness Effects on the Tip Vortex Strength and Cavitation Inception*, Sixth International Symposium on Marine Propulsors: smp19, Rome, Italy, May 2019.

[8] Tapia, X.P. *Modelling of wind flow over complex terrain using OpenFoam*, Master thesis, University of Gavle, 2009.